ORIGINAL RESEARCH

RIG-I Promotes Cell Death in Hepatocellular Carcinoma by Inducing M1 Polarization of Perineal Macrophages Through the RIG-I/MAVS/NF-κB Pathway

Bei Zhou
Cuiping Li
Yun Yang
Zhuo Wang

Department of Biochemistry and Molecular Biology, School of Basic Medical Sciences, Xinxiang Medical University, Xinxiang, Henan 453003, People's Republic of China

Background: The development and metastasis of cancer cells are regulated by tumor-associated macrophages (TAMs) present in the surrounding tumor microenvironment. RIG-I is a key pathogen recognition receptor against RNA viruses that regulates innate immunity in cancer progression. Till now, the mechanism of RIG-I regulation of the polarization of TAMs in the progression of hepatocellular carcinoma (HCC) has not been understood.

Materials and Methods: Levels of RIG-I and the key proteins in the NF-κB pathway in HCC and paired paracancerous tissues were detected by Western blotting. The transfection efficiency of RIG-I was observed by fluorescence microscopy. The M1 and M2 markers were detected by real-time polymerase chain reaction and FACS assays. Apoptosis of RIG-I lentivirus-infected HCC cells was detected by flow cytometry assay. Death of Hepa1-6 and H22 cells was analyzed by lactate dehydrogenase releasing assay.

Results: The level of RIG-I was decreased in HCC tissues as compared to that in the paired paracancerous tissues. Overexpression of RIG-I in mouse peritoneal macrophages increased the expression of the biomarkers CD16/32 and CD11c associated with M1 macrophages. The relative levels of IL-1β, TNF-α, IL-6, and iNOS were significantly increased in RIG-I lentivirus-infected macrophages, whereas the levels of Arg-1 and IL-10 were not significantly different in RIG-I-overexpressed peritoneal macrophages. Moreover, overexpression of RIG-I in peritoneal macrophages promoted apoptosis of Hepa1-6 and H22 cells. Furthermore, overexpression of RIG-I increased the levels of phosphorylated p65 and p-IκB and decreased the level of IκB in peritoneal macrophages. Importantly, the expression of MAVS and TRAF2 was significantly increased in RIG-I lentivirus-infected macrophages.

Conclusion: Our results demonstrate that overexpression of RIG-I promoted apoptosis and death of HCC cells. Moreover, RIG-I promoted the polarization of M1 through the RIG-I/MAVS/TRAF2/NF-κB pathway in mice peritoneal macrophages, suggesting that RIG-I may be a novel target in the immunotherapy of HCC.

Keywords: RIG-I, M1 macrophages, hepatocellular carcinoma, cell apoptosis, NF-κB pathway

Introduction

Primary liver carcinoma is a common malignant tumor in China.[1] Surgery is the main treatment method followed by comprehensive treatment, in combination with chemotherapy, radiotherapy, and immunotherapy.[2] However, liver carcinoma is often diagnosed in the late stage, when radical surgery is not an option. Thus,

Correspondence: Bei Zhou
Email zhoubeiwork@163.com

chemotherapy is an important adjuvant treatment for liver cancer. Although liver cancer cells are sensitive to chemotherapeutic drugs, they are prone to multidrug resistance (MDR), which is a recurrent problem in the treatment of liver cancer.[3] Despite several advances made in the treatment of these tumors, the frequent recurrence and distant metastases make the development of new therapies urgent and necessary.[4]

The occurrence and tumorigenesis of liver carcinoma is a complex and variable process. The clinical progress of immunotherapy has been extremely rapid.[5] There are now many kinds of immunological checkpoint inhibitor drugs being used.[6,7] Tumor microenvironment refers to the internal environment created in cancer nest tissues during the tumor progression. In the tumor microenvironment, there are various cell types including tumor cells themselves, mesenchymal cells, tumor-related immune cells, tumor microvessels, tumor stromal cells, together with tissue fluid, cytokines, etc.[8] Macrophages are important immune cells that present high plasticity and heterogeneity and can transform into different polarization states under different microenvironments. M1 and M2 macrophages are the two main activated macrophages.[9] The M1 phenotype is characterized by high levels of cluster of differentiation (CD) 86, CD16/32, and CD11c.[9] Moreover, some proinflammatory factors such as interleukin (IL)-6, IL-1β, and tumor necrosis factor (TNF)-α are also highly expressed in M1 macrophages. M1 macrophages are typically activated by interferon (IFN)-γ and lipopolysaccharide (LPS), an inducer of exogenous TNF or a product of bacteria. The activated M2 macrophages normally secret IL-10 and CD206, among others. The regulation of the differentiation of tumor-associated macrophages in the tumor microenvironment is important for antitumor immunity.[10] Thus, it is urgent and meaningful to find the effective agents participating in the polarization of macrophages during cancer progression.

Retinoic acid-inducible gene I (RIG-I)-like receptors (RLRs) such as RIG-I, melanoma differentiation-associated protein 5 (MDA5), and lipophosphoglycan biosynthetic protein 2 (LGP2) are important pathogen recognition receptors involved in the defense against RNA viruses. RIG-I and MDA5 together promote M1 macrophage polarization in vivo in response to West Nile virus infection.[11] In the hepatoma cell line, LH86, RIG-I responds to hepatitis C virus by inducing IFN and apoptosis to activate innate immunity.[12] It has been reported that the activation of RNA agonists of RIG-I greatly improves the effects of cancer immunotherapy.[13] The activation of RIG-I in cancers without viral infection may be a better choice to induce immunogenic tumor cell death and increase cytotoxic activity of lymphocytes in tumor microenvironment.[14] However, the role of RIG-I in cellular immunity and tumor microenvironment is still unclear. Thus, in the present study, we explored the role of RIG-I in the polarization of macrophages and its potential use in immunotherapy through targeting components of the tumor microenvironment of hepatocellular carcinoma (HCC).

Materials and Methods
Clinical Specimens
Patients were recruited from the First Affiliated Hospital of Xinxiang Medical University. The institutional approval number for human studies is 2,016,024. A total of 12 patients were included in the study and appropriately informed. All the patients signed the relevant consent contracts prior to the study. The research carried out on humans was in compliance with the Helsinki Declaration. The 12 HCC specimen samples were collected from June 2016 to September 2018. The median age of the patients was 59.3 years (range: 28–79 years). None of the patients underwent anticancer treatment before operation. Fresh tumor tissues were collected from the patients. The tumor specimens and noncancerous tissues were quickly frozen at −80°C prior to Western blotting analysis and real-time polymerase chain reaction (PCR) assays.

Cell Lines and Reagents
The THP-1, L02, RAW 264.7, Hepa1-6, and H22 cells were purchased from ATCC and cultured in Dulbecco's modified Eagle's medium (DMEM; Hyclone Corporation, Logan, Utah, USA) containing 10% fetal bovine serum (FBS; Hyclone Corporation) at 37°C in a 5% CO_2-containing atmosphere. Ddx58 (NM_172689) Mouse Tagged ORF Clone Lentiviral Particle (CAT＃: MR226477L4V) and Lenti ORF control particles of pLenti-C-mGFP-P2A-Puro (CAT＃: PS100093V) were purchased from Origene Corporation. Total RNA extraction kit (MK700) was purchased from TaKaRa corporation. The cDNA reverse transcription kit (6110) was obtained from TaKaRa. Lipofectamine 2000 (cat. no. 11668–019) was obtained from Invitrogen.

Isolation of Mouse Peritoneal Macrophages

The mice were sacrificed by cervical dislocation, and the abdominal skin was cut. Then, 5–10 mL of sterile phosphate-buffered saline (PBS) was injected into the upper part of the abdominal cavity with a syringe. The abdomen was massaged several times, and the PBS in the mouse abdomen was aspirated. The cells were collected by centrifugation at $400 \times g$ for 10 min and plated on a 6-cm plate in DMEM supplemented with 10% FBS. After an overnight incubation, the medium and the cells that were not adhered to the plate were aspirated, and the remaining cells were washed with PBS and replaced with the new DMEM containing 10% FBS and streptomycin double antibody. All cells were cultured at 37°C in a 5% CO_2 atmosphere.

Flow Cytometric Analysis

Annexin V-fluorescein isothiocyanate (FITC) staining was used to analyze the apoptosis of osteosarcoma cells, according to previously published protocols.[15] The purity and phenotype markers of peritoneal macrophages were analyzed by FACS with phycoerythrin (PE)-conjugated anti-F4/80, FITC-conjugated anti-CD11c, and PE-conjugated anti-mouse CD16/32 antibodies. The information of the antibodies used is as follows: PE-conjugated anti-F4/80 is a monoclonal antibody (BM8) and was purchased from eBioscience (cat. no. 12-4801-80). FITC-conjugated anti-CD11c is a monoclonal antibody (N418) and was purchased from eBioscience (cat. no. 11–0114-82). PE-conjugated anti-mouse CD16/32 antibody was purchased from BioLegend corporation (cat. no. 101307). Briefly, 1×10^6 Hepa1-6 or H22 cells were washed twice in cold PBS. The PE-conjugated or FITC-conjugated antibodies were added to a final concentration of 100 ng/mL each. The antibodies were incubated for 20 min at 4°C in the dark, prior to flow cytometry analysis (FACScan; Belgium).

RNA Preparation and RT-PCR

Total RNA isolation was performed with RNApure kit (Bioteke, China). Total RNA samples were retrotranscribed with MLV-reverse transcriptase (Invitrogen, USA). RNA specimens and corresponding cDNA samples were preserved at −80°C. Quantitative PCR was performed using ABI Prism 7500 as follows: 40 cycles of 95°C for 12 s and 58°C for 30 s. All PCR reactions were

performed in triplicate. β-actin was used as the internal reference for normalization. Primers used were as follows:

RIG-I: 5′-GCATATTGACTGGACGTGGCA-3′ and 5′-CAGTCATGGCTGCAGTTCTGTC-3′

β-actin: 5′-AGAGGGAAATCGTGCGTGAC-3′ and 5′-CAATAGTGATGACCTGGCCGT-3′

IL-1β: 5′-TCATTGTGGCTGTGGAGAAG-3′ and 5′-AGGCCACAGGTATTTTGTCG-3′

TNF-α: 5′-CATCTTCTCAAAATTCGAGTGACAA-3′ and 5′-TGGGAGTAGACAAGGTACAACCC-3′

IL-6: 5′-ATCCAGTTGCCTTCTTCTTGGGACTGA -3′ and 5′-TAAGCCTCCGAC TTGTGAAGTGGT-3′

iNOS: 5′-CTGCAGCACTTGGATCAGGAACCTG-3′ and 5′-GGAGTAGCCTGTGTGCACCTGGAA-3′

Arg-1: 5′-CAGAAGAATGGAAGAGTCAG-3′ and 5′-CAGATATGCAGGGAGTCACC-3′

IL-10: 5′-GCTCTTACTGACTGGCATGAG-3′ and 5′-CGCAGCT-CTAGGAGCATGTG-3′

Western Blotting

Cell lysates were prepared and separated by polyacrylamide gel electrophoresis (PAGE) as previously described.[16–18] The antibodies used are as follows: anti-RIG-I/DDX58 antibody (cat. no. ab45428) is a rabbit polyclonal antibody tested in mouse, rat, and human, which was obtained from Abcam. Anti-MAVS antibody (cat. no. ab189109) is a rabbit polyclonal antibody and was purchased from Abcam. Anti-TRAF2 *Homo sapiens* TNF receptor-associated factor 2 (TRAF2) (cat. no. TA319201) is a rabbit polyclonal antibody and was purchased from OriGene (Beijing, China), and the dilution was 1 μg/mL. Recombinant anti-TRAF3 antibody [EPR22992-93] (cat. no. ab239357) is a rabbit monoclonal antibody and was purchased from Abcam. Anti-Phospho-NF-kappaB p65 (Ser536) antibody (cat. no. 3031) was purchased from Cell Signaling technology. Anti-NFκB p65 antibody (F-6) (cat. no. sc-8008) is a mouse monoclonal immunoglobulin (Ig) G1 and was purchased from Santa Cruz Biotechnology, and the concentration was 200 μg/mL. Recombinant anti-IKB alpha (phospho S36) antibody [EPR6235(2)] (cat. no. ab133462) is a rabbit monoclonal antibody and was purchased from Abcam. Anti-IκB -α antibody (cat. no. AI096) is a rabbit polyclonal antibody and was purchased from Beyotime, with a dilution of 1:1000. Mouse monoclonal anti-β-actin antibody (Cat. No. TA310155) was obtained from OriGene. Goat anti-rabbit IgG-HRP (Cat. No. sc-2004) and goat anti-mouse IgG-HRP (sc-2005) were obtained from Santa Cruz. The

quantification of Western blotting was used Image J software.

Lactate Dehydrogenase (LDH) Assay

The peritoneal macrophages were obtained as indicated above. RIG-I lentivirus-infected macrophages or negative control lentivirus-infected macrophages were used as effector cells. Hepa1-6 or H22 cells were used as targeted cells. One hundred microliters of hepa1-6 or H22 cells (1×10^4 cells per well) and 100 μL of effector cells at the effector: target ratio of 5:1, 10:1 or 20:1 were incubated for 24 h in Roswell Park Memorial Institute 1640 medium containing 2% FCS. Twenty-four hours later, the cells were centrifugated at $400 \times g$ for 10 min, 100 μL of the supernatant was transferred to 96-well flat-bottom plates, and lysis of target cells was determined by measuring LDH release with a kit (KeyGentec Company, Nanjing, China). The experiments were performed in triplicate and repeated twice.

Mice Group and Tumor Challenge

Male 6–8-week old C57BL/6 mice were cultured in micro-isolator cages. They were handled under aseptic conditions following the approved protocol of the Institutional Animal Care and Use Committee (IACUC) of Xinxiang Medical University. The mice were randomly assigned to three groups. Each group contained eight mice. The mice in each group were intraperitoneally (i.p.) inoculated with H22 (1×10^6 cells) suspended in 200 μL PBS. Two days later, the mice in each group were intraperitoneally (i.p.) inoculated with 5×10^6 cells suspended in 200 μL PBS. All studies involving mice were approved by the Animal Study Committee. Survival following the tumor challenge was recorded.

Statistical Analysis

All data were analyzed using SPSS software. Student's t-tests were used to evaluate statistical significance. Results are depicted as means ± standard deviation (SD). Values of $p < 0.05$ were defined as statistically significant.

Results
The Level of RIG-I is Decreased in Patients with Clinical HCC

To test the role of RIG-I in the progression of HCC, the expression level of RIG-I was detected by RT-PCR in a cohort of 12 clinical HCC specimens and their paired paracancerous tissues. As shown in Figure 1, the RT-PCR results showed that the levels of RIG-I at the mRNA level

were significantly decreased in HCC tissues as compared to that in the paired paracancerous tissues (**$p < 0.01$). Additionally, Western blotting was performed to verify the results from RT-PCR assay. Among them, the levels of RIG-I at the protein level were detected in four pairs of HCC tissues and the paired paracancerous tissues. The results from Western blotting analysis were consistent with the data obtained by RT-PCR assay.

Overexpression of RIG-I by Lentivirus System Promotes M1 Polarization in vitro in Mouse Peritoneal Macrophages

Next, we investigated whether overexpression of RIG-I affected the polarization of M1 or M2 macrophages. Peritoneal macrophages were obtained from mice. As shown in Figure 2, the purity of isolated macrophages was tested by FACS assay, and the cell rate with F4/80 marker was 94.36%. Then, the macrophages were infected with RIG-I lentivirus or negative control lentivirus for 48 hours. The transfection efficiency was observed by fluorescence microscopy at 400 X magnification. The biomarkers of M1 macrophages, CD16/32 and CD11c, were also tested by FACS assay, and the positive rate of both markers was 81.76% in RIG-I overexpressed macrophages (Figure 2C). These data suggest that overexpression of RIG-I by lentivirus increased the abundance of M1 macrophages.

Furthermore, the relative expression of M1 markers such as IL-1β, TNF-α, IL-6, and inducible nitric oxide synthase (iNOS) was significantly increased in RIG-I lentivirus-infected peritoneal macrophages as compared to that of negative control lentivirus-infected macrophages (**$p < 0.01$). Additionally, the expression of M2 markers such as Arg-1 and IL-10 was not significantly different in RIG-I lentivirus-infected peritoneal macrophages as compared to that of the negative control (Figure 3). The above-mentioned data show that overexpression of RIG-I promoted polarization of M1 macrophages.

Overexpression of RIG-I in Peritoneal Macrophages Promotes Apoptosis and Death of Human and Mouse Liver Cancer Cells

To test whether overexpression of RIG-I affects the apoptosis of liver cancer cells, Annexin V-FITC/PI staining was analyzed by FACS. The mouse liver hepatoma Hepa1-6 cells, from the mice peritoneal macrophages infected with
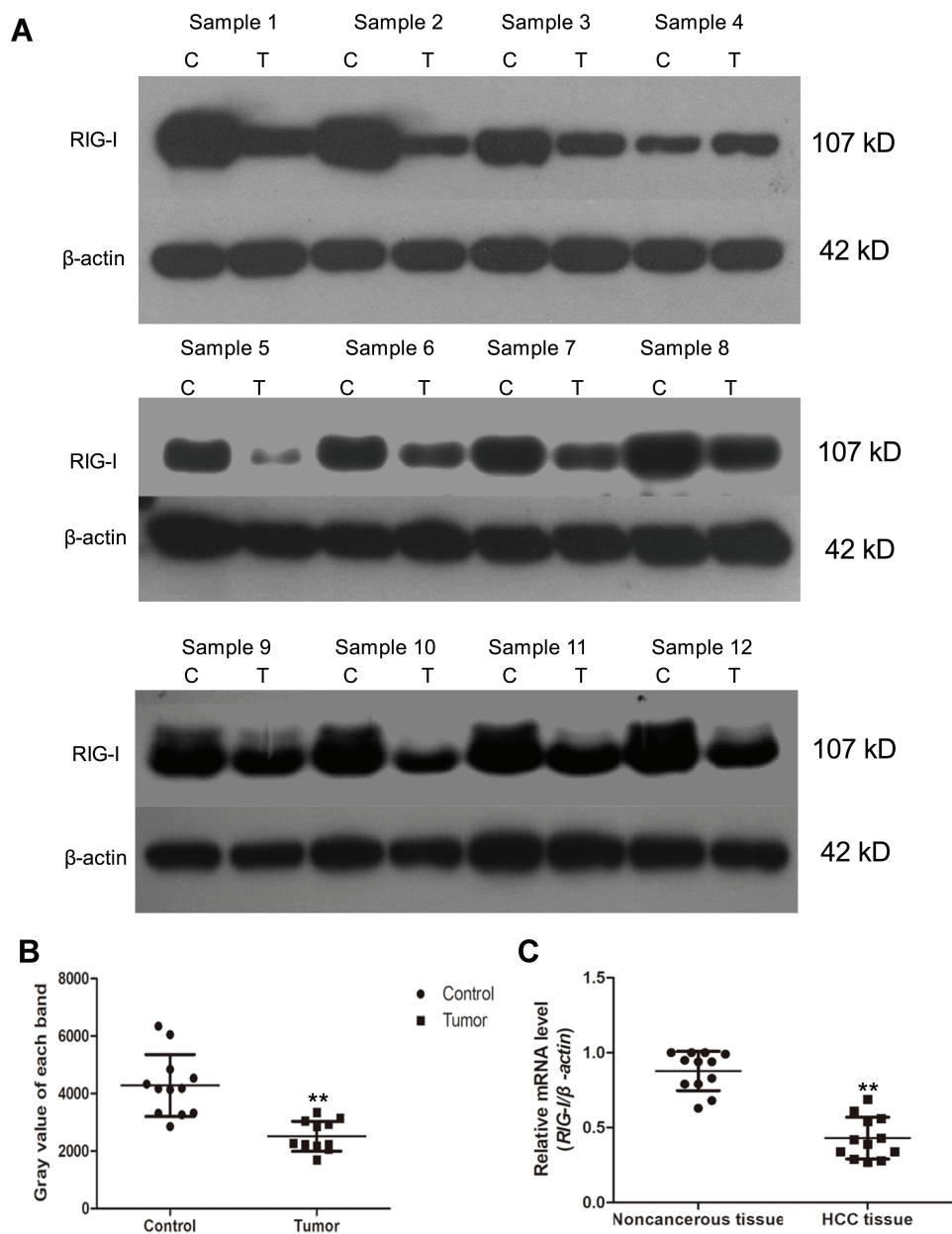
A

Figure 1 The level of RIG-I is decreased in human clinical hepatic carcinoma (HCC) patients. (**A**) Twelve pairs of HCC specimens and its paired paracancerous specimens were collected. The levels of RIG-I were detected by Western blotting analysis. (C) control tissues referred to the paracancerous tissues; (T) tumor tissues, that is the HCC specimens. (**B**) The levels of RIG-I in noncancerous tissues and HCC tissues were shown in scatter-plot. Beta-actin was used as internal reference gene. **p<0.01, compared with noncancerous tissues. (**C**) RT-PCR assay. The relative mRNA level of RIG-I was shown in scatter-plot in a cohort of 12 HCC specimens and its paired noncancerous tissues. **p<0.01, compared with noncancerous tissues.

RIG-I lentivirus or negative control lentivirus for 48 hours, were cultured in conditioned medium. As shown in Figure 4, the apoptosis rate was significantly increased in the Hepa1-6 cells treated with the conditioned medium from RIG-I overexpressing macrophages compared with that of negative control lentivirus-infected peritoneal macrophages. This was consistent in the mouse liver cancer cell H22. The apoptotic rate of H22 cells was up to 32.71% with the conditioned medium from RIG-I

overexpressing macrophages, significantly higher than that with the conditioned medium from negative control lentivirus-infected macrophages, which was 12.86% (**$p < 0.01$). Moreover, the apoptosis of SMMC7721 and HepG2 cells with the conditioned medium from RIG-I lentivirus-infected macrophages were significantly higher than that of the cells with the conditioned medium from negative control lentivirus-infected THP-1-derived macrophages (**$p < 0.01$). These results demonstrate
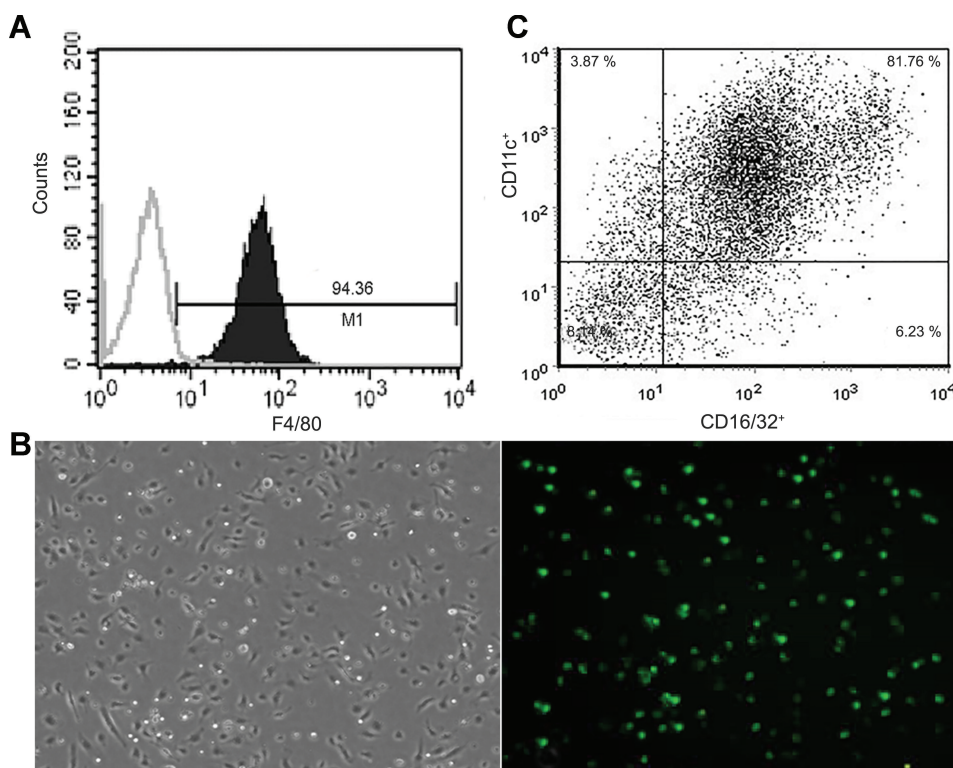
Figure 2 Overexpression of RIG-I by lentivirus system in mouse peritoneal macrophage promoted M1 polarization in vitro. (**A**) Identification of the purity of isolated peritoneal macrophages in mice by FACS. (**B**) The mouse peritoneal macrophages were collected and transfected with RIG-I lentivirus for 72h. The transfection efficiency of RIG-I was observed by fluorescence microscope ×400. (**C**) FACS assay was used to evaluate expression of the biomarker CD16/32 and CD11c associated with M1.
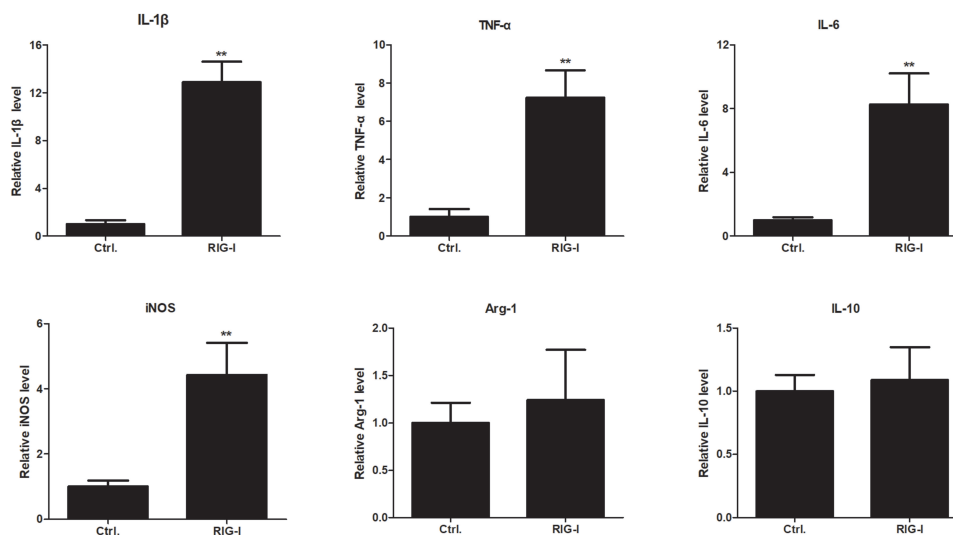
Figure 3 Peritoneal macrophages in mice were infected with RIG-I lentivirus or negative control lentivirus and were subsequently treated with 100ng/mL LPS and 20ng/mL IFN-γ for 24 hours. Real-time PCR assay was performed to test the relative level of IL-1β, TNF-α, IL-6, iNOS, Arg-1 and IL-10 in peritoneal macrophages. **p<0.01, compared with control lentivirus-transfected cells.

that the apoptosis rate of liver hepatoma cells was obviously increased by conditioned medium generated from RIG-I lentivirus-infected macrophages.

Additionally, cell death was also tested by measuring LDH release into the culture medium of the damaged HCC

mice cells by LDH assay. As shown in Figure 5, the levels of LDH were significantly higher in Hepa1-6 and H22 cells cultured with the conditioned medium from RIG-I overexpressing macrophages than that from negative control lentivirus-infected macrophages (**$p < 0.01$). Consistently, in
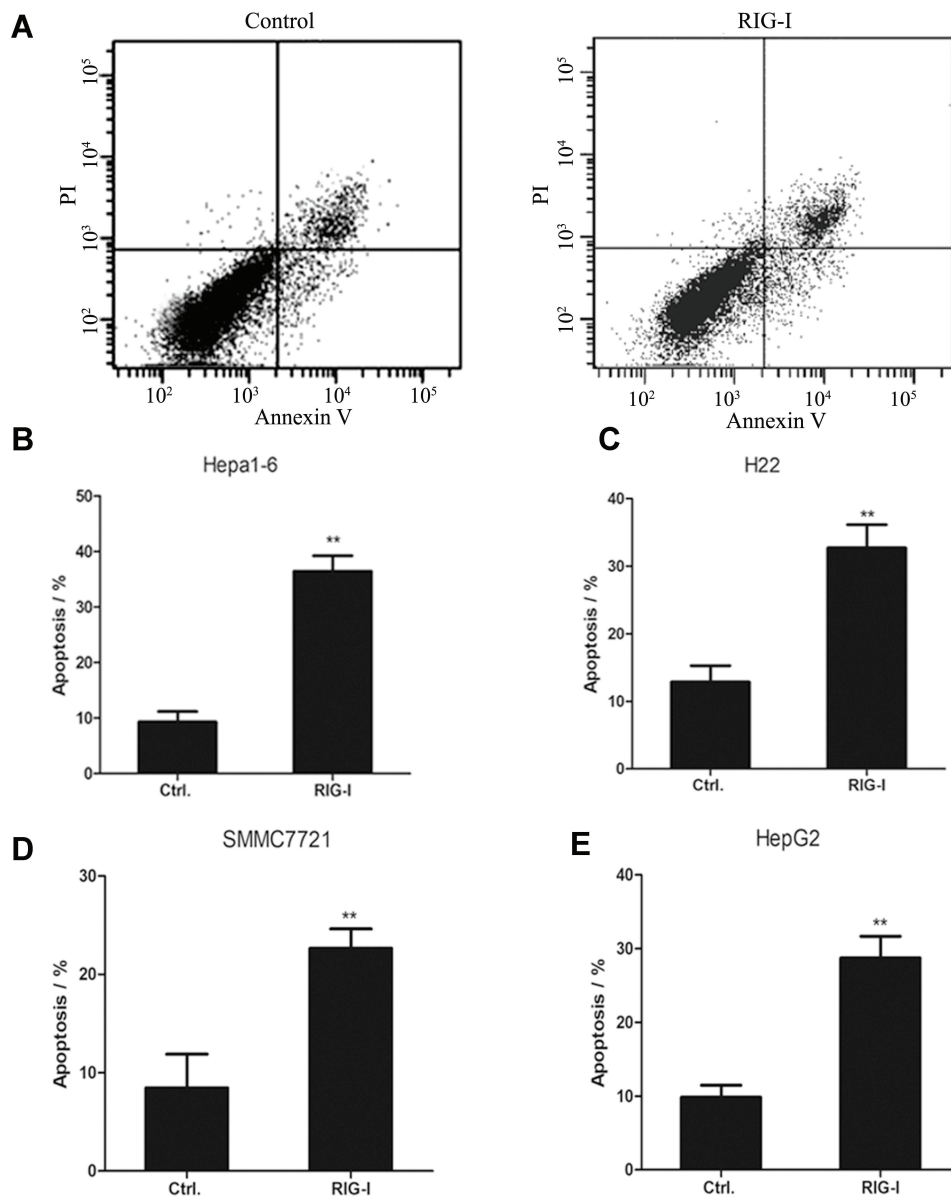
Figure 4 Overexpression of RIG-I in mouse and human macrophages promoted cell apoptosis of the corresponding liver cancer cells. (**A**) Hepa1-6 cells were cultured with conditioned medium from peritoneal macrophages infected with RIG-I lentivirus or negative control lentivirus. After 48 hours, FACS assay was performed to test the cell apoptosis of Hepa1-6 cells with Annexin V-FITC/PI staining method. (**B**) The apoptosis rate of Hepa1-6 cells cultured with conditioned medium was shown in histogram. **p<0.01, between the groups with conditioned medium from peritoneal macrophages infected with RIG-I lentivirus or negative control lentivirus. (**C**) The apoptosis rate of H22 cells was shown in histogram. **p<0.01, between the groups with conditioned medium from peritoneal macrophages infected with RIG-I lentivirus or negative control lentivirus. (**D**) The apoptosis rate of SMMC7721 cells cultured with conditioned medium was shown in histogram. **p<0.01, between the groups with conditioned medium from THP-1 derived macrophages infected with RIG-I lentivirus or negative control lentivirus. (**E**) The apoptosis rate of HepG2 cells was shown in histogram. **p<0.01, between the groups with conditioned medium from THP-1 derived macrophages infected with RIG-I lentivirus or negative control lentivirus.

human liver cancer cells SMMC7721 and HepG2, the group with the conditioned medium from RIG-I lentivirus-infected macrophages had higher levels of LDH than that of negative control lentivirus-infected macrophages (**$p < 0.01$). All the data suggest that overexpression of RIG-I in macrophages promoted death of mice HCC cells such as Hepa1-6 and H22 cells and human HCC cells such as SMMC7721 and HepG2 cells by promoting the polarization of M1 macrophages.

Overexpression of RIG-I in Human THP1-Induced Macrophages has No Effect on Cell Death of Normal Hepatocytes

Furthermore, we wanted to investigate whether overexpression of RIG-I in macrophages affects cell death of normal hepatocytes by analyzing PI staining with FACS assay. Here,
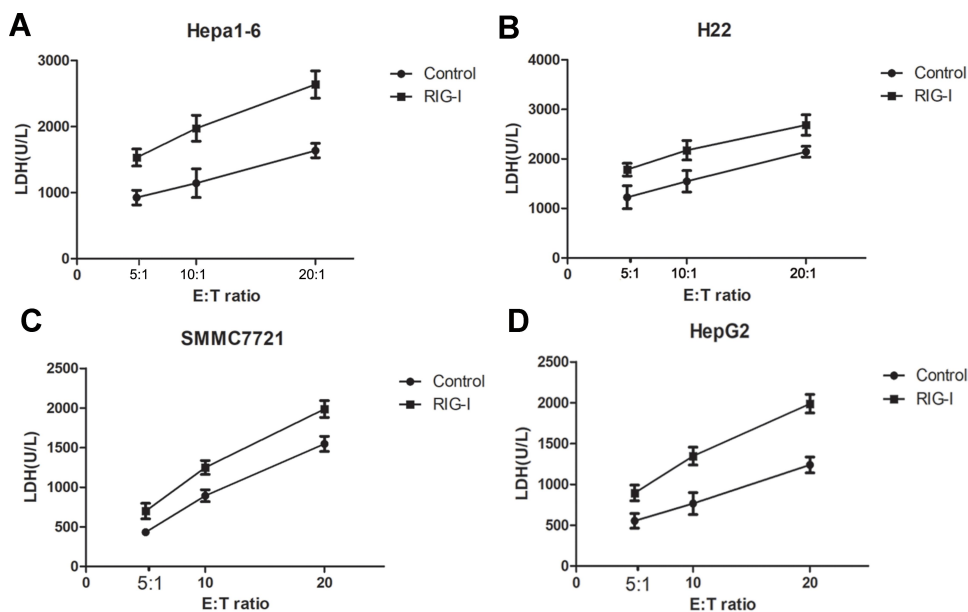
Figure 5 RIG-I promotes cell death of Hepa1-6, H22, SMMC7721 and HepG2 cells. The peritoneal macrophages were infected with RIG-I lentivirus or negative control lentivirus for 48 hours. LDH release assays were performed with the RIG-I lentivirus-infected macrophages or negative control lentivirus-infected macrophages as effector cells and Hepa1-6 cells (**A**), H22 cells (**B**), SMMC7721 (**C**) and HepG2 (**D**) as target cells. The effector-to-target cells ratios were 5:1, 10:1 and 20:1. The experiments were performed in triplicate and repeated twice.

we used the conditioned medium from RIG-I lentivirus-infected THP-1-derived macrophages or control lentivirus-infected THP-1-derived macrophages to culture the normal human hepatocytes L02 cells. As shown in Figure 6, there was no significant difference between the cell death rates of RIG-I lentivirus-infected macrophages (5.73%) and control lentivirus-infected macrophages (3.96%). The results show that over-expression of RIG-I in human THP1-induced macrophages has no effect on cell death of normal hepatocytes.

Overexpression of RIG-I Activates NF-κB Pathway in Macrophages

It was reported that the activation of NF-κB signaling pathway contributes to the polarization of M1 macrophages. Here, we

explored the relationship between RIG-I overexpression and NF-κB pathway in peritoneal macrophages. As shown in Figure 7, phosphorylation of p65 and IκB was obviously upregulated in RIG-I overexpressing macrophages as compared to that of vector-transfected macrophages. Moreover, the level of IκB was significantly decreased in RIG-I lentivirus-infected peritoneal macrophages after LPS and IFN-γ treatment. This suggests that overexpression of RIG-I activated the NF-κB signaling pathway in peritoneal macrophages.

As shown in Figure 7, the NF-κB and RIGI/MAVS signaling pathways were activated in peritoneal macrophages after LPS and IFN-γ treatment, confirming the previous result. Specifically, the peritoneal macrophages were treated
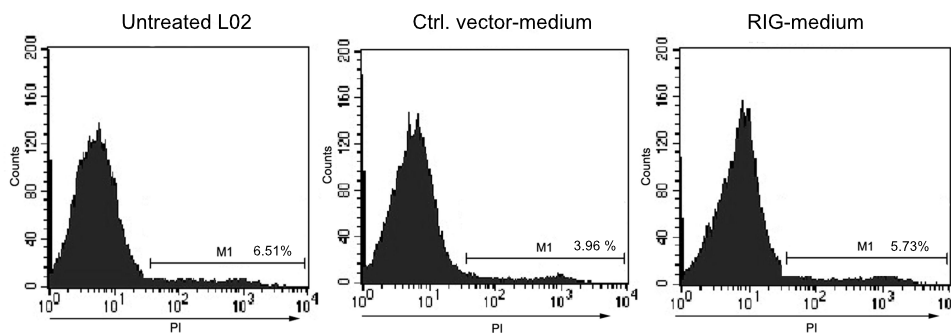

Figure 6 Over-expression of RIG-I in human THP1-induced macrophages has no effects on cell death in normal hepatocytes. The conditioned medium from RIG-I lentivirus-infected THP-1-derived macrophages or control lentivirus-infected THP-1-derived macrophages to culture the normal human hepatocytes L02 cells. Cell death of RIG-I lentivirus-infected macrophages, control lentivirus-infected macrophages and untreated control L02 cells were tested by FACS assay with PI staining.
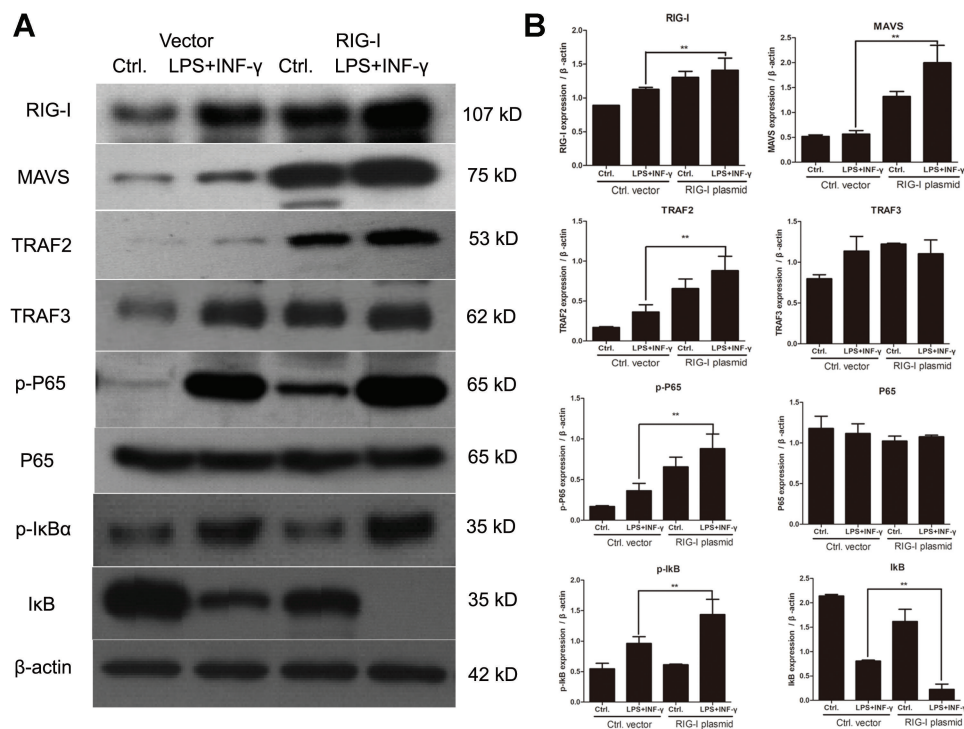
Figure 7 Overexpression of RIG-I activates NF-κB pathway in macrophages. (**A**) Peritoneal macrophages were infected with RIG-I lentivirus or negative control lentivirus and subsequently treated with 100 ng/mL LPS and 20 ng/mL IFN-γ for 24 hours. The levels of RIG-I, MAVS, TRAF2, TRAF3, p65 and IκBα were detected by Western blotting, as well as the phosphorylated p65 and IκBα. (**B**) The gray value of each band was analyzed with Image J software. The expression of RIG-I, MAVS, TRAF2, TRAF3, p65 and IκBα were shown in histogram. **p<0.01, compared with control group.

with LPS in combination with IFN-γ for 24 hours. MAVS and TRAF2 were highly expressed in RIG-I lentivirus-infected macrophages. However, the expression of TRAF3 was not obviously different in RIG-I lentivirus-infected macrophages. The above-mentioned findings reveal that RIG-I activated the NF-κB signaling pathway by RIG-I/MAVS/TRAF2 pathway.

RIG-I-Induced M1 Suppresses in vivo Tumor Growth

Furthermore, to detect in vivo antitumor effects of RIG-I-induced M1 macrophages, H22 liver cancer cells were inoculated into C57BL/6 mice. The mice were randomly divided into three groups and intraperitoneally injected with 1×10^6 H22 cells in PBS buffer. Two days later, RIG-I-transfected RAW 264.7 cells and control vector-transfected RAW 264.7 cells were intraperitoneally inoculated into each group of mice. Then, the mice were kept and cultured to observe the formation of ascites in each group. As shown in Figure 8, RIG-I-transfected RAW 264.7 cells inhibited the ascites formed by H22 cells as compared to that of the control group. The survival proportion of RIG-I-transfected RAW 264.7 group was significantly higher than that of vector-transfected RAW 264.7 and PBS groups.

Discussion

Due to the high plasticity of macrophages, the cells can change from one polarization state to another under different microenvironments and transcription factors.[19,20] Several reports show that RIG-I mediates antiviral responses in the innate immune system, but recent studies found that RIG-I is also activated in the absence of viral infection. The antitumor effects of RIG-I were reported in several human cancers such as pancreatic cancer,[21] gastric cancer,[22] colorectal cancer,[23] glioblastoma,[24] prostate cancer,[25] etc., and also applied in cancer therapy.[13,14,26] The present study mainly focused on the effects of RIG-I on M1 macrophage differentiation and its antitumor effects in HCC cells.

First, we found a decrease in expression levels of RIG-I in 10 of a cohort of 12 (83.3%) clinical HCC specimens compared with that of its paired paracancerous tissues both by RT-PCR and Western blotting. Our results show that RIG-I served as a tumor suppressor in the progression of HCC. Activation of RIG-I related pathways by radiation or chemotherapy was proved to generate a favorable outcome in patients with cancer.[27]

Next, we explored the effects of RIG-I in tumor micro-environment for therapeutic cancer treatment. Macrophages
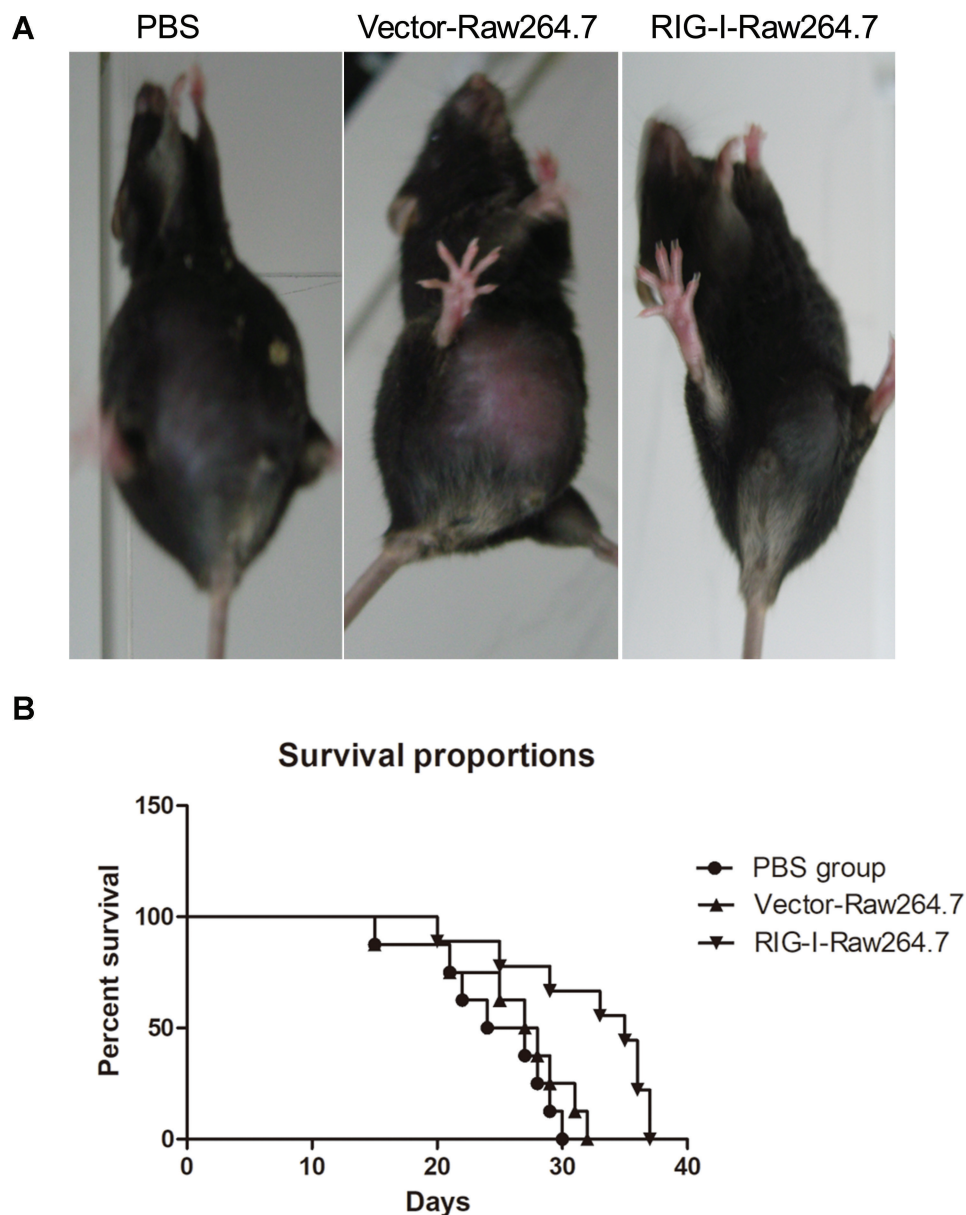
Figure 8 RIG-I induced M1 suppresses in vivo tumor growth. Male 6–8-week old C57BL/6 mice were treated as described in Material and Method. (**A**) After 3-week of inoculation, the representative mouse in each group was photographed. (**B**) Survival proportions in three groups were shown.

play a key role in many diseases including infection, cancer, autoimmunity, and atherosclerosis.[28] Their main function is to protect against pathogens and mediate tissue repairing.[29] The plasticity of M1 and M2 macrophages allows these opposite polarity types to provide primary host protection and maintain tissue homeostasis.[30] M1 macrophages are thought to produce proinflammatory cytokines and possess antimicrobial and tumor-killing activities. M2 macrophages are involved in immunosuppression, tumorigenesis, wound repair, and parasitic elimination.[31] M1 macrophages are usually induced by microbial products and proinflammatory cytokines and toxic effector molecules such as IL-1β, IL-6,

IL-12, TNF-α, nitric oxide (NO), reactive oxygen species (ROS), and especially IFN-γ, which kills intracellular pathogens including viruses, infected cells, or tumor cells. In addition to cellular responses, the complement cascade factor secreted by M1 macrophages and the expression of high levels of MHC class I and class II molecules enhance the adaptive immune response to tumor cells.[32] Here, we found that the overexpression of RIG-I promoted the polarization of M1 macrophages in vitro. More importantly, the RIG-I induced M1 macrophages cocultured with HCC cells significantly increased apoptosis and death of HCC cells from mice. The in vivo tumor-bearing assay also showed that RIG-I

transfected RAW 264.7 cells inhibited the ascites formed by H22 cells and enhanced the tumor-bearing survival time of mice as compared to that of the control group.

The NF-κB family signaling pathway plays a vital role in tumor progression and metastasis. Normally, the IκB inhibitory proteins bind to the NF-κB family and remain in the cell matrix, which is not activated.[33] When external stimuli activate the NF-κB pathway, IκB kinase (IKK) phosphorylates the IκB inhibitory protein of the NF-κB family, leading to its inactivation and dissociation into the nucleus of the NF-κB nuclear transcription factor.[33,34] It has been shown that over-expression of RIG-I activates NF-κB.[35,36] Here, we further confirmed that the overexpression of RIG-I activates NF-κB pathway in macrophages through the RIG-I/MAVS/TRAF2 pathway.

In conclusion, overexpression of RIG-I promoted apoptosis and death of HCC cells, probably due to the polarization of M1 through the RIG-I/MAVS/TRAF2/NF-κB pathway in mice peritoneal macrophages, suggesting that RIG-I can have an important role in the immunotherapy of HCC.

Disclosure

The authors report no conflicts of interest for this work.

References

1. Xiao YB, Zhang B, Wu YL. Radiofrequency ablation versus hepatic resection for breast cancer liver metastasis: a systematic review and meta-analysis. *J Zhejiang Univ Sci B*. 2018;19(11):829–843. doi:10.1631/jzus.B1700516
2. VoPham T, Bertrand KA, Hart JE, et al. Pesticide exposure and liver cancer: a review. *Cancer Causes Control*. 2017;28(3):177–190. doi:10.1007/s10552-017-0854-6
3. Marin JJG, Briz O, Herraez E, et al. Molecular bases of the poor response of liver cancer to chemotherapy. *Clin Res Hepatol Gastroenterol*. 2018;42(3):182–192. doi:10.1016/j.clinre.2017.12.006
4. Wang Y, Shen L, Lu M, Ji Z, Zhang X. Multimodality treatment including triplet regimen as first-line chemotherapy may improve prognosis of serum AFP-elevated gastric cancer with liver metastasis. *Gastroenterol Res Pract*. 2017;2017:5080361. doi:10.1155/2017/5080361
5. Greten TF, Sangro B. Targets for immunotherapy of liver cancer. *J Hepatol*. 2017.
6. Ou DL, Lin YY, Hsu CL, et al. Development of a PD-L1-expressing orthotopic liver cancer model: implications for immunotherapy for hepatocellular carcinoma. *Liver Cancer*. 2019;8(3):155–171. doi:10.1159/000489318
7. Long L, Zhang X, Chen F, et al. The promising immune checkpoint LAG-3: from tumor microenvironment to cancer immunotherapy. *Genes Cancer*. 2018;9(5–6):176–189.
8. Frankel T, Lanfranca MP, Zou W. The role of tumor microenvironment in cancer immunotherapy. *Adv Exp Med Biol*. 2017;1036:51–64.
9. Nagarsheth N, Wicha MS, Zou W. Chemokines in the cancer microenvironment and their relevance in cancer immunotherapy. *Nat Rev Immunol*. 2017;17(9):559–572. doi:10.1038/nri.2017.49
10. Wang D, Jiang W, Zhu F, Mao X, Agrawal S. Modulation of the tumor microenvironment by intratumoral administration of IMO-2125, a novel TLR9 agonist, for cancer immunotherapy. *Int J Oncol*. 2018;53(3):1193–1203. doi:10.3892/ijo.2018.4456
11. Stone AEL, Green R, Wilkins C, Hemann EA, Gale M Jr. RIG-I-like receptors direct inflammatory macrophage polarization against West Nile virus infection. *Nat Commun*. 2019;10(1):3649. doi:10.1038/s41467-019-11250-5
12. Eksioglu EA, Zhu H, Bayouth L, et al. Characterization of HCV interactions with Toll-like receptors and RIG-I in liver cells. *PLoS One*. 2011;6(6):e21186. doi:10.1371/journal.pone.0021186
13. Jacobson ME, Wang-Bishop L, Becker KW, Wilson JT. Delivery of 5′-triphosphate RNA with endosomolytic nanoparticles potently activates RIG-I to improve cancer immunotherapy. *Biomater Sci*. 2019;7(2):547–559. doi:10.1039/C8BM01064A
14. Elion DL, Cook RS, Harnessing RIG. I and intrinsic immunity in the tumor microenvironment for therapeutic cancer treatment. *Oncotarget*. 2018;9(48):29007–29017. doi:10.18632/oncotarget.25626
15. Hussain AR, Khan AS, Ahmed SO, et al. Apigenin induces apoptosis via downregulation of S-phase kinase-associated protein 2-mediated induction of p27Kip1 in primary effusion lymphoma cells. *Cell Prolif*. 2010;43(2):170–183. doi:10.1111/j.1365-2184.2009.00662.x
16. Nishitani H, Sugimoto N, Roukos V, et al. Two E3 ubiquitin ligases, SCF-Skp2 and DDB1-Cul4, target human Cdt1 for proteolysis. *EMBO J*. 2006;25(5):1126–1136. doi:10.1038/sj.emboj.7601002
17. Peng L, Xu Z, Zhou Y, Yang T, Liang ZQ, Zhang M. [Effect of rosiglitazone on cells cycle, apoptosis and expression of Skp2 and p27Kip1 in hepatocellular carcinoma cell line]. *Zhonghua Gan Zang Bing Za Zhi*. 2010;18(2):148–149. doi:10.3760/cma.j.issn.1007-3418.2010.02.017
18. Schulman BA, Carrano AC, Jeffrey PD, et al. Insights into SCF ubiquitin ligases from the structure of the Skp1-Skp2 complex. *Nature*. 2000;408(6810):381–386. doi:10.1038/35042620
19. Gajewski TF, Woo SR, Zha Y, et al. Cancer immunotherapy strategies based on overcoming barriers within the tumor microenvironment. *Curr Opin Immunol*. 2013;25(2):268–276. doi:10.1016/j.coi.2013.02.009
20. Noman MZ, Hasmim M, Lequeux A, et al. Improving cancer immunotherapy by targeting the hypoxic tumor microenvironment: new opportunities and challenges. *Cells*. 2019;8:9. doi:10.3390/cells8091083
21. Zillinger T, Hartmann G. Targeted nanoparticle delivery of bifunctional RIG-I agonists to pancreatic cancer. *Mol Ther*. 2019;27(3):491–492. doi:10.1016/j.ymthe.2019.02.005
22. Chen L, Feng J, Wu S, et al. Decreased RIG-I expression is associated with poor prognosis and promotes cell invasion in human gastric cancer. *Cancer Cell Int*. 2018;18:144. doi:10.1186/s12935-018-0639-3
23. Zhu H, Xu WY, Hu Z, et al. RNA virus receptor Rig-I monitors gut microbiota and inhibits colitis-associated colorectal cancer. *J Exp Clin Cancer Res*. 2017;36(1):2. doi:10.1186/s13046-016-0471-3
24. Glas M, Coch C, Trageser D, et al. Targeting the cytosolic innate immune receptors RIG-I and MDA5 effectively counteracts cancer cell heterogeneity in glioblastoma. *Stem Cells*. 2013;31(6):1064–1074. doi:10.1002/stem.1350
25. Kato T, Ueda Y, Kinoh H, et al. RIG-I helicase-independent pathway in sendai virus-activated dendritic cells is critical for preventing lung metastasis of AT6.3 prostate cancer. *Neoplasia*. 2010;12(11):906–914. doi:10.1593/neo.10732
26. Wu Y, Wu X, Wu L, Wang X, Liu Z. The anticancer functions of RIG-I-like receptors, RIG-I and MDA5, and their applications in cancer therapy. *Transl Res*. 2017;190:51–60. doi:10.1016/j.trsl.2017.08.004
27. Ranoa DR, Parekh AD, Pitroda SP, et al. Cancer therapies activate RIG-I-like receptor pathway through endogenous non-coding RNAs. *Oncotarget*. 2016;7(18):26496–26515. doi:10.18632/oncotarget.8420

28. Vitale I, Manic G, Coussens LM, Kroemer G, Galluzzi L. Macrophages and metabolism in the tumor microenvironment. *Cell Metab*. 2019;30(1):36–50. doi:10.1016/j.cmet.2019.06.001

29. Bose D, Banerjee S, Chatterjee N, Das S, Saha M, Saha KD. Inhibition of TGF-beta induced lipid droplets switches M2 macrophages to M1 phenotype. *Toxicol in Vitro*. 2019;58:207–214. doi:10.1016/j.tiv.2019.03.037

30. Nie W, Yu T, Sang Y, Gao X. Tumor-promoting effect of IL-23 in mammary cancer mediated by infiltration of M2 macrophages and neutrophils in tumor microenvironment. *Biochem Biophys Res Commun*. 2017;482(4):1400–1406. doi:10.1016/j.bbrc.2016.12.048

31. Kim H, Wang SY, Kwak G, Yang Y, Kwon IC, Kim SH. Exosome-guided phenotypic switch of M1 to M2 macrophages for cutaneous wound healing. *Advan Sci*. 2019;6(20):1900513. doi:10.1002/advs.201900513

32. Monteiro LN, Rodrigues MA, Gomes DA, Salgado BS, Cassali GD. Tumour-associated macrophages: relation with progression and invasiveness, and assessment of M1/M2 macrophages in canine mammary tumours. *Veterinary J*. 2018;234:119–125. doi:10.1016/j.tvjl.2018.02.016

33. Lee H, Lee DS, Chang KJ, Kim SH, Cheong SH. Ribose-taurine suppresses inflammation through NF-kappaB regulation in activated RAW 264.7 macrophages. *Adv Exp Med Biol*. 2019;1155:1057–1067.

34. Sun P, Sun N, Yin W, et al. Matrine inhibits IL-1beta secretion in primary porcine alveolar macrophages through the MyD88/NF-kappaB pathway and NLRP3 inflammasome. *Vet Res*. 2019;50(1):53. doi:10.1186/s13567-019-0671-x

35. Zheng B, Wang X, Liu Y, et al. Japanese Encephalitis Virus infection induces inflammation of swine testis through RIG-I-NF-kB signaling pathway. *Vet Microbiol*. 2019;238:108430. doi:10.1016/j.vetmic.2019.108430

36. Zhou HJ, Li H, Shi MQ, et al. Protective effect of klotho against ischemic brain injury is associated with inhibition of RIG-I/NF-kappaB signaling. *Front Pharmacol*. 2017;8:950. doi:10.3389/fphar.2017.00950